



A cost-effective method for obtaining single magnetic cotton yarns

Iuliana G. Lupu, Marian C. Grosu, Oana Cramariuc, Florin Tudorache, Daniela C. Nastac & Horatiu I. Hogas

To cite this article: Iuliana G. Lupu, Marian C. Grosu, Oana Cramariuc, Florin Tudorache, Daniela C. Nastac & Horatiu I. Hogas (2021): A cost-effective method for obtaining single magnetic cotton yarns, The Journal of The Textile Institute, DOI: [10.1080/00405000.2021.1989819](https://doi.org/10.1080/00405000.2021.1989819)

To link to this article: <https://doi.org/10.1080/00405000.2021.1989819>



© 2021 The Author(s). Published by Informa UK Limited, trading as Taylor & Francis Group



Published online: 03 Nov 2021.



Submit your article to this journal [↗](#)



Article views: 131



View related articles [↗](#)



View Crossmark data [↗](#)

A cost-effective method for obtaining single magnetic cotton yarns

Iuliana G. Lupu^a, Marian C. Grosu^b, Oana Cramariuc^{c,d}, Florin Tudorache^e, Daniela C. Nastac^c and Horatiu I. Hogas^f

^aDepartment of Textile Products Engineering and Design, Gh. Asachi Technical University Iasi, Iasi, Romania; ^bNational R&D Institute for Textile and Leather, Bucharest, Romania; ^cIT Center for Science and Technology, Bucharest, Romania; ^dDepartment of Physics, Tampere University, Tampere, Finland; ^eInterdisciplinary Research, Science Research Department, A.I. Cuza University of Iasi, Romania; ^fDepartment of Land Measurements and Cadastre, Gh. Asachi Technical University Iasi, Iasi, Romania

ABSTRACT

In this work, we propose a cost-effective procedure to obtain magnetic single cotton yarns by employing commercially available magnetic powders and adhesives. Two different indirect magnetization methods are used on the yarns coated with several mixtures containing barium hexaferrite ($\text{BaFe}_{12}\text{O}_{19}$) as hard magnetic powder. The BH mass percentage is varied between 10% and 50%. Specific textile coating binders such as polyurethane and polyvinyl acetate are used as adhesives. A constant amount of 5% glycerol is employed as plasticizer agent. An in-house developed laboratory equipment is used to produce the magnetic cotton yarns. The equipment allows primary orientation of the magnetic particles along external field lines and subsequent magnetization until saturation. Our studies show that the diameter of the coated yarns is directly dependent on the amount of magnetic powder in the coating solution. Thus, the magnetic yarn diameter increases by 30% when compared to the 356 μm diameter of the reference (uncoated) yarn for a barium hexaferrite mass percentage of 50%. Also, our studies reveal that increasing the magnetic properties (residual magnetism and coercive field intensity) of the composite yarns is possible only by increasing the mass percentage of the magnetic powder content. The highest values of the magnetic properties have been measured when neodymium permanent magnets (NdFeB) were used for the magnetization instead of a toroidal coil. The residual magnetization and saturation increase with the amount of barium hexaferrite embedded in the textile yarn. However, the increase in mass percentage is limited by the degradation of the yarn properties which allow them to be used for textile applications. SEM images of the coated yarns reveal a relatively uniform deposition of magnetic layer on the reference cotton yarn.

ARTICLE HISTORY

Received 13 April 2021
Accepted 1 October 2021

KEYWORDS

Magnetic yarns; barium hexaferrite; electromagnetic coil; permanent magnets; tensile and magnetic characteristics

Introduction

Smart textiles combine, in a powerful and efficient way, different textile and non-textile elements. Among these, magnetic textiles have emerged as a less usual but quite interesting form of smart textile with a wide range of envisaged applications in the field of medical treatment, electronic textiles, smart clothing, sportswear, biomedicine or protective clothing. Magnetic fabric is used by companies such as Green Grace¹ in the United States to promote healing at a cellular level. Magnetic coils with a textile core can be built as described by Zieba et al. (Zieba, 2007). Another important application is in wave absorption and electromagnetic shielding (Akman et al., 2013) for protective clothing. Furthermore, the magnetic properties of magnetic yarns can be combined with other microsensors which may be used in applications such as antennas and soft keyboards (Jia et al., 2019, Ghosh et al., 2018, Loss et al., 2019, Xu et al., 2018). Overall, magnetic textiles are used for electronic devices and circuits, sensors and actuators, theft and data security tags,

intelligent clothing for monitoring of human physiological parameters.

Magnetic textile products have some similar characteristics with classical magnetic materials (Akşit et al., 2009; Bartusch et al., 2014; Campos et al., 2011). The magnetic yarn can receive micro and nano magnetic functionalities (Wiak et al., 2010; 2012) by various methods of production such as: spinning of natural and metallic continuously/staple fibers passing through a magnetic field with variable induction (Zieba et al., 2011); spinning of cellulosic magnetic fibers containing ferromagnetic and/or ferromagnetic micro powders (Rubacha & Zięba, 2006); production of single magnetic continuous fibers by coating of diamagnetic yarns with magnetic solutions made of ferromagnetic and/or ferromagnetic micro powders which are fixed on the backing material with a binder. A wide range of support yarns (e.g. carded, combed, simple and twisted monofilamentary and polyfilamentary, fully drawn yarns) can be used to tune their properties and application area.

CONTACT Oana Cramariuc  oana.cramariuc@tuni.fi

© 2021 The Author(s). Published by Informa UK Limited, trading as Taylor & Francis Group
This is an Open Access article distributed under the terms of the Creative Commons Attribution-NonCommercial-NoDerivatives License (<http://creativecommons.org/licenses/by-nc-nd/4.0/>), which permits non-commercial re-use, distribution, and reproduction in any medium, provided the original work is properly cited, and is not altered, transformed, or built upon in any way.

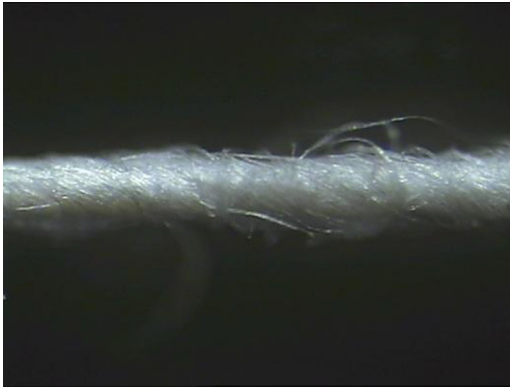


Figure 1. Microscope image of reference yarn.

In a previous work we studied the effect of two process variables on the magnetic properties of *twisted cotton yarns made of combed single staple yarns* covered with *hard ferro-magnetic powder* by using a central composite design to determine the optimal processing factors that can affect the magnetic properties of the fibers (Grosu et al., 2016). The cotton yarns were magnetized by incorporating magnetic particles and by passing the yarn through an electromagnetic coil. Our results showed that an increase in ferrite content is influencing the saturation and residual induction of cotton twisted staple yarns. The magnetic properties can be optimized not only through the selection of the ferrite content but also by varying the current intensity through the electromagnetic coil used for magnetization.

In another study we fabricated and characterized similar magnetic *twisted cotton yarns made of combed single staple yarns* in terms of magnetic, tensile and bending properties (Grosu et al., 2018). Both hard and soft magnetic powder coatings were deposited on the yarns. The magnetic and tensile properties of the magnetic yarns increased with the increase in magnetic powder content for a given magnetic material. Bending properties were influenced by the magnetic material type and by the adhesive content in the coating. For example, a higher number of cracks were exhibited by the hard magnetic yarns compared to the soft ones.

In this paper we study a *single cotton carded yarn* and a hard magnetic powder mixed with specific textile coating binders (polyurethane resin – PUR – adhesives and polyvinyl acetate – PVAc) for the production of magnetic yarns (Aldib, 2015; Bashir et al., 2011; Beica et al., 2008; Chowdhury et al., 2013; Hemapriyamvadha & Sivasankar, 2015; Kang et al., 2011; Kobya et al., 2014). The choice of a carded yarn was made because it exhibits protruding surface fibers which improve the adherence of the magnetic powder (Grosu et al., 2018). This was proven in our previous studies to be an important factor affecting the properties of the magnetic yarns. Also, based on previous studies, we increased the range of the hard magnetic powder content in the coating mixture. We used different mixtures of hard magnetic powder to cover the yarns which were then magnetized using two different indirect magnetization methods (Joseph & Stupak, 2000). Indirect magnetization methods involve the use of intense external magnetic fields to induce magnetic excitation in the material. These methods involve

Table 1. Samples codes and corresponding mass percentage.

Sample codes	BaFe ₁₂ O ₁₉ , wt.%
Y1	10
Y2	20
Y3	30
Y4	40
Y5	50

the use of: (i) electrical conductors placed axially, in the sample, (ii) permanent magnets placed nearby the sample, (iii) electromagnets placed nearby the sample, in order to generate high magnetic inductions or (iv) solenoids, in this latter case the sample for magnetization is placed longitudinally in the concentrated magnetic field and fills the center of the coil or solenoid.

The tensile and magnetic properties of the resulting magnetic cotton yarns are investigated and discussed. The aim was to obtain magnetic single yarns through a cost-effective procedure which involves commercially available magnetic powders and adhesives, and to study which of the two indirect magnetization methods used in this study can provide higher values of residual and saturation magnetization.

Materials and methods

Materials

In this investigation, the reference yarn used as reinforcing diamagnetic element was a 100% cotton carded *single* yarn with Z twist direction, 600 twist/m and a fineness of 55.5 tex. This type of yarn was chosen because of the following properties: (i) its cross section is almost circular; (ii) being a carded yarn, there are many fibers (hairs) standing out from the yarn surface and (iii) the high number of twists/m ensures enough strength for the yarn to withstand tensioning during the covering process. The optical image of the reference yarn as obtained by an Olympus SZX10 microscope set to a 9.5 zoom factor is given in Figure 1.

Based on insight from previous research (Grosu et al., 2016; 2018) where we studied magnetic *twisted* cotton yarns, several mixtures containing barium hexaferrite (BaFe₁₂O₁₉) as hard magnetic powder were chosen to cover the cotton *single* yarn. We used barium hexaferrite with a mass percentage between 10% and 50%, two polymers in liquid state (polyvinyl acetate and polyurethane) and glycerol. The barium hexaferrite was supplied by Rofep, Romania. It is a hexagonal hard magnet with magnetoplumbite structure widely used as ceramic permanent magnet. Its basic characteristics were presented in our previous study (Grosu et al., 2018).

The binding adhesives were mixed with the magnetic powder prior to fiber coating. Polyvinyl acetate, a widely used thermoplastic adhesive, has a good adherence to cellulosic materials. Also, polyurethane (7% mass percentage) has a remarkable adherence when used as adhesive. Glycerol was used as plasticizer agent for the blends and the amount was kept constant at 5%. The coated samples codes and corresponding mass percentage of magnetic powder in the mixtures are listed in Table 1.

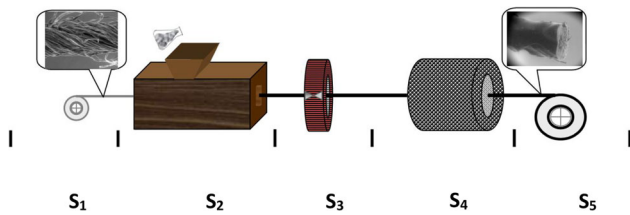


Figure 2. Schematic drawing of the equipment employed in obtaining of the magnetic in which the following elements are depicted: S_1 – yarn supply system, S_2 – feeding, transport, storage, coating and solution calibration system, S_3 – magnetizing system; S_4 – heating and fixing of coated yarn system, S_5 – yarn winding system.

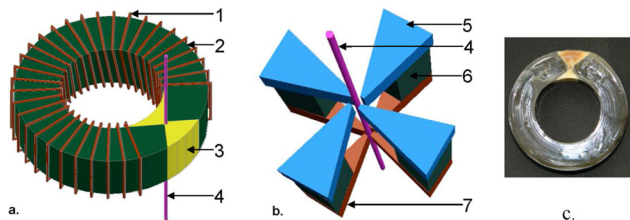


Figure 3. Magnetization devices used after yarn coating: a. toroidal coil, b. magnetic auger die, c. ferromagnetic core (real image) where: (1) copper coils, (2) ferromagnetic core, (3) air gap, (4) coated yarn, (5) polar angles positioned offset from the axis of the yarn; (6) NdFeB permanent magnets; (7) polar angles positioned centrally on the axis of the yarn.

Methods

Preparation of magnetic yarns

An in-house developed laboratory equipment, schematically depicted in Figure 2, was used for coating the cotton yarns with magnetic powder. The equipment allows for the primary orientation of the magnetic particles along the field lines of a 0.14 T external magnetic field. After coating, the yarn was subjected to a more powerful magnetization until saturation. The device comprises five sub-systems: S_1 – yarn supply system, S_2 – feeding, transport, storage, coating and solution calibration system, S_3 – magnetizing system; S_4 – heating and fixing of coated yarn system, S_5 – yarn winding system.

The deposition process occurs in the magnetic mixture feed chamber which is equipped with a special calibration device of spinneret type with a circular hole 500 μm in diameter, which ensures a uniform deposition of the polymer mixture. After calibration, the coated yarn passes through the magnetic device placed in S_3 for indirect magnetization.

The first magnetization method employs a toroidal induction coil with electromagnetic excitation (Figure 3a). The coil is powered by a DC source of 10 V and 10 A.

The ferromagnetic core of the coil is X-shaped. The gap is filled with an epoxy resin (see Figure 3c) with a small cylindrical channel through which the yarn coated with barium hexaferrite passes at a speed that allows magnetization until saturation of the ferrimagnetic particles that make up the coated magnetic layer. Measurements of the magnetic field intensity of the coil were performed by using a Koshava 5, Wuntronic Teslameter equipped with a transversal Hall probe placed in the air gap (Figure 4), before filling it with the resin (which doesn't affect the magnetic field).

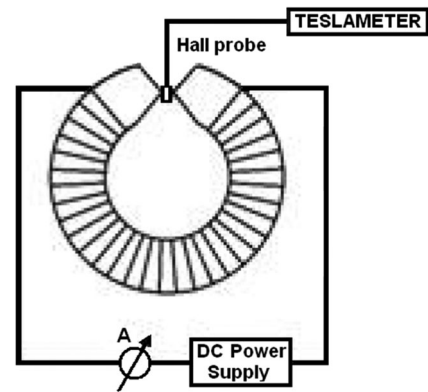


Figure 4. Layout of the measuring equipment of magnetic induction in the coil.

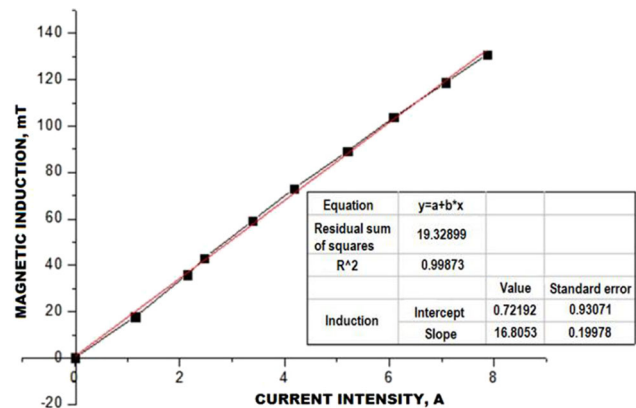


Figure 5. Dependency of coil induction on current intensity.

We used linear regression in order to evaluate the dependency between current intensity and the induction of the coil's magnetic field. The results are presented in Figure 5. For current intensities up to about 8 A the induction increases linearly with the current. The value of the correlation coefficient being nearly 1 illustrates a very good correlation.

The second magnetization method employed a hybrid type magnetic device (see Figure 3b) made of rare earth trapezoidal permanent neodymium iron boron magnets (NdFeB) disposed diametrically opposed on a circle. The permanent magnets contain two sets of four soft magnetic pieces having high permeability and a triangular shape with polar angles ('auger' configuration). The magnetic field is perpendicular on the yarn and is concentrated by the magnetic device polar angles. Measurements of the magnetic field of the magnetic auger die were performed in the same way as described above for the toroid. In order to close the field line, the Hall probe tip was successively positioned between each of the eight polar angles. The measured magnetic induction between adjacent magnetic poles was approximately 0.7 T (see Figure 6).

This measured value indicates the major advantage of the magnetic auger die regarding production cost and multipolar magnetization compared to the electromagnetic coil. Each of the magnetization methods was separately employed on the samples mentioned in Table 1.

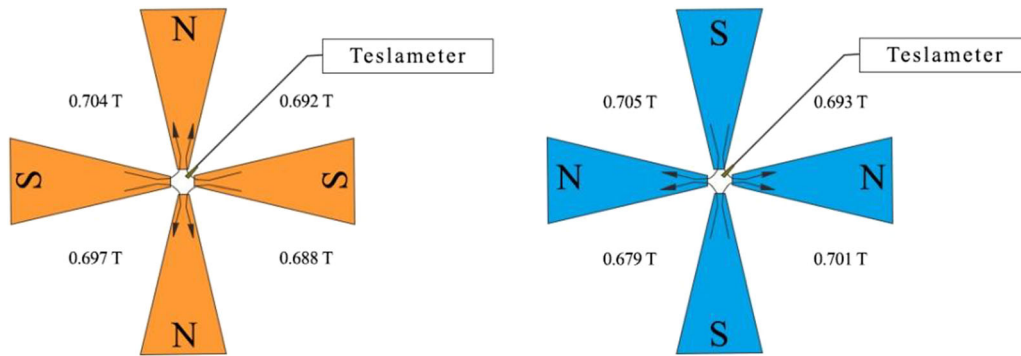


Figure 6. Magnetic induction measuring layout of magnetic auger die: a. front view, b. rear view.

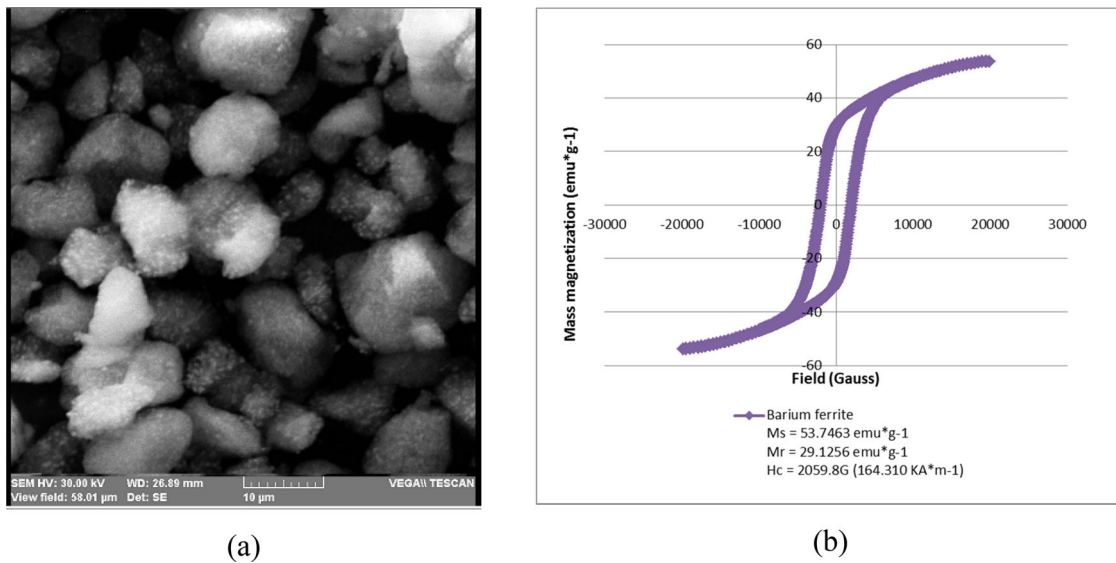


Figure 7. (a) SEM image of barium hexaferrite, (b) hysteresis loop of the magnetic powder.

Diameter measurements

The magnetic sample yarns were conditioned in a standard atmosphere of $65\% \pm 2\%$ RH and at room temperature ($20^\circ \pm 2^\circ\text{C}$) in order to investigate the diameter and magnetic properties. The apparent diameter of the reference yarn and magnetic yarns was measured using a Projectina Neerbrugg microscope with a 20x magnification. The diameter values were further used to estimate the thickness of the coating layer, which is very difficult to determine directly because the thin polymer film is deposited on the uneven surface of the cotton yarn. Consequently, the thickness was calculated according to the relation:

$$T = d_{MY} - d_0 \quad (1)$$

where: d_{MY} – magnetic yarn diameter in μm ; d_0 – uncoated yarn diameter in μm .

SEM (Scanning Electron Microscopy) micrographs of the magnetic yarns covered with barium hexaferrite in various concentrations were carried out at room temperature using a FEI Quanta 200 scanning electron microscope equipped with a GSED detector.

Tensile properties measurements

Yarn tensile properties are also an important parameter for the practical processing of coated yarns in woven or knitting

fabrics. Therefore, the magnetic yarns were tested for their tensile properties on a Tinius Olsen H5KT SDL Atlas tensile machine using a 250 mm gage length and an 80 mm/min cross-head speed (according to SR EN ISO 2062). The values of breaking force and elongation were obtained by performing 10 tests for each yarn sample.

Magnetic properties measurements

The measurements of magnetic properties of the composite yarns were performed by using a vibrating sample magnetometer Lake Shore 7300 capable of a maximum magnetic induction of 2 T in the temperature range 4 K – 1300 K. The hysteresis loops were measured according to the ASTM A894/A894M-00 (2011) e1.

Results and discussions

Based on our previous study (Grosu et al., 2018), the SEM image of the barium hexaferrite powder obtained using an SEM-EDX model VEGA II LSH TESCAN and the hysteresis loop that was performed by using a Magnetic field Meter MAG-ST100 are given in Figure 7a and b, respectively. M_s

is the saturation magnetization, M_r is the residual magnetization and H_c the intensity of coercive field.

Using scanning electron microscopy, the average barium hexaferrite particle size was found to be 0.94 μm . The distribution histogram of barium hexaferrite particle size is shown in Figure 8 based on 50 samples. The microparticle diameters ranged from 0.54 μm to 1.64 μm .

In order to verify the barium hexaferrite stoichiometry, the percentage composition of the compounds was determined using energy-dispersive X-ray (EDX) spectrometry. The details of the composition are shown in Figure 9 and Table 1. All the elements are well resolved using the K- and L-shell X-rays with few artifacts (Figure 9). Figure 9 is revealing that Fe is the highest energy element in the barium hexaferrite compound with 6.41 keV on the K-shell. Barium has 4.83 keV on the L-shell.

Based on previous research (Grosu et al., 2018), the weight and atomic percent of Fe are about 89% and 76%, respectively, while barium ferrite has 4% and 1.3%, as shown in Table 2. This composition is in agreement with the theoretical stoichiometry of the compound.

The hard magnetic powder was also characterized by means of X-ray diffraction (XRD) at room temperature using the Cu K_{α} line with a rate of 3°/min (Shimadzu LabX XRD-6000). The X-ray diffraction pattern is presented in Figure 10. The interplanar spacings and relative intensities determined from the diffraction pattern were compared with those of the ICDD published data for barium hexaferrite (PDF card 84-0757) and iron (III) oxide, hematite (PDF card 33-0664) compounds.

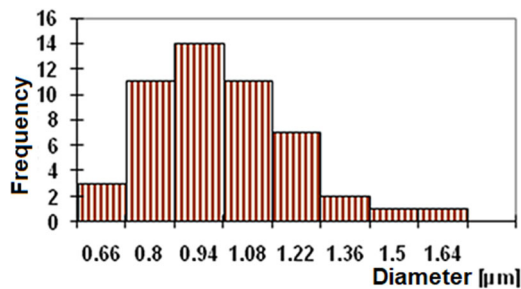


Figure 8. Distribution histogram of BHF particle size.

As shown in Figure 10 the particles were proven to be a mixture of hexagonal $\text{BaFe}_{12}\text{O}_{19}$ and trigonal Fe_2O_3 , similar results being reported in the literature by other authors (Grosu et al., 2018; Petrila & Tudorache, 2014; Sözeri et al., 2012; Vinnik et al., 2015). The sharp peaks observed in the X-ray diffraction pattern confirm the high crystallinity of the phases. SEM photographs showed that the products consist of particles with a relatively narrow size distribution, as can be observed from Figure 8. This also was confirmed in all cases by XRD patterns.

SEM micrographs of uncoated yarn coded as Y0 and composite yarns coded as Y1 ÷ Y5 covered with $\text{BaFe}_{12}\text{O}_{19}$ in various concentrations are presented in Figure 11. The images in Figure 11b are evidencing the effect of the coating solution on the thin polymer magnetic layer built around the surface of the reference yarn Y0 (Figure 11a). Higher

Table 2. Barium hexaferrite composition obtained from EDX spectrometry (see also Figure 9).

Element	Number (AN)	Line	keV	Weight (%)	Atomic(%)
Fe	26	K	6.41	88.54	75.71
O	8	K	0.0096	7.70	22.98
Ba	56	L	4.83	3.76	1.31
Total				100	100

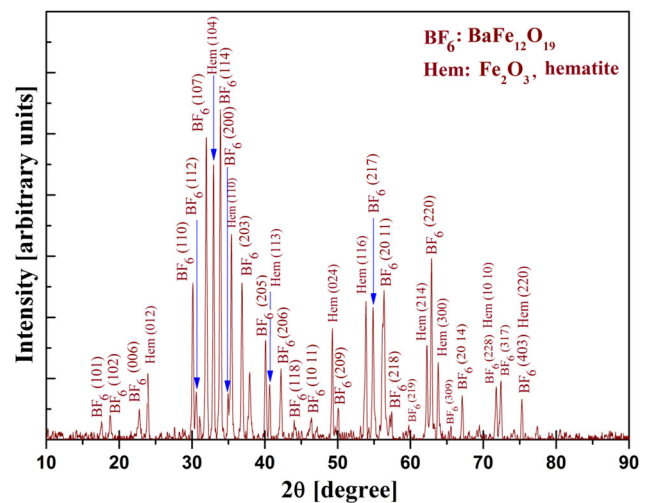


Figure 10. XRD pattern of barium hexaferrite.

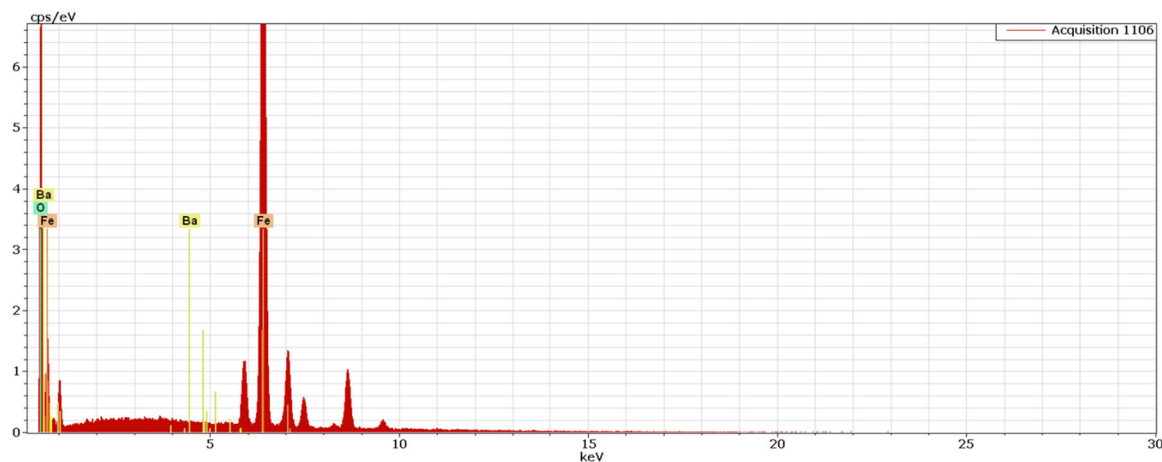
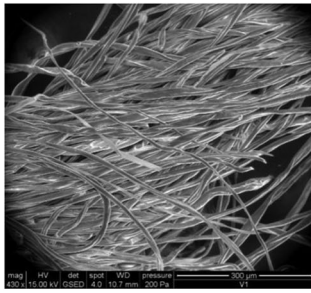
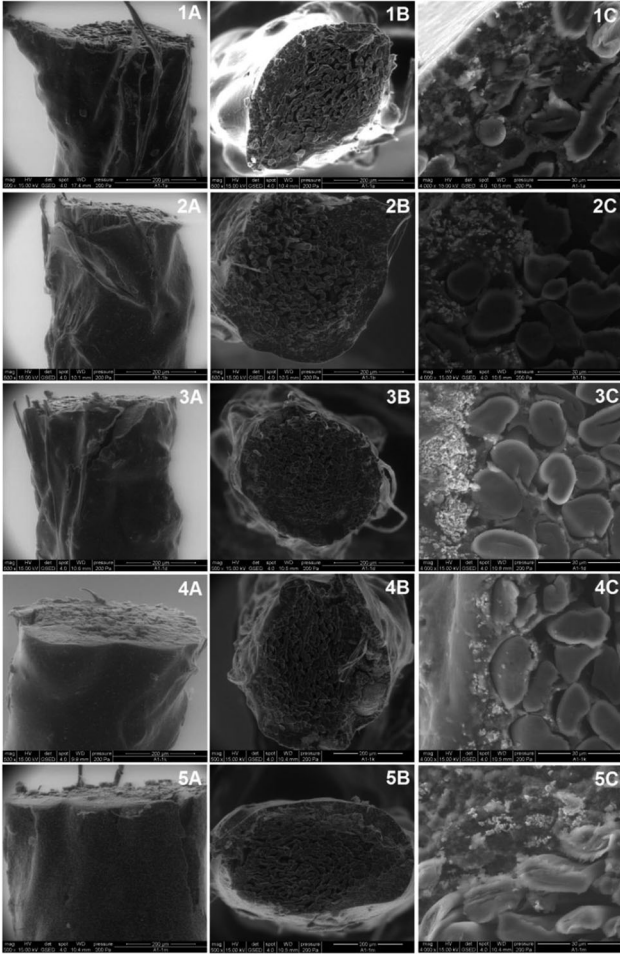


Figure 9. Spectrum of barium ferrite powder collected at 30 keV using EDX equipment.



a.



b.

Figure 11. SEM images of composite yarns: a. Y0, b. Y1 ÷ Y5: A – side view of samples; B – cross section view; C – zoomed cross section.

Table 3. Structural modifications of magnetic yarns vs. reference yarn.

Samples codes	Type of core	Average diameter d(μm)	Magnetic layer thickness T(μm)
Y0	100% cotton	356	–
Y1		427	71
Y2		438	82
Y3		445	89
Y4		457	101
Y5		465	109

concentrations of magnetic coating solution increase the thickness of the coating layer.

Table 3 shows the experimental average values of the reference yarn (Y0) and composite yarn diameter (Y1 ÷ Y5) as well as the magnetic layer thickness at the yarn surface.

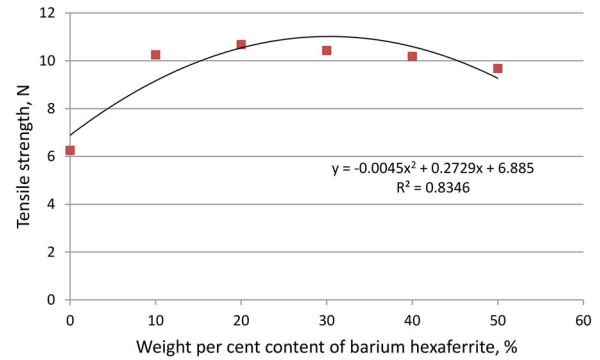


Figure 12. Dependency of magnetic yarns tensile strength on barium hexaferrite content.

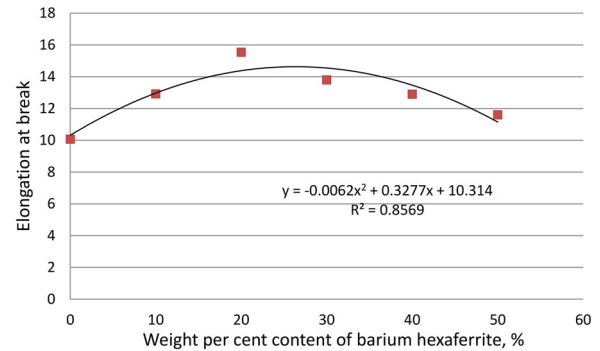


Figure 13. Dependency of magnetic yarns elongation at (%) on barium hexaferrite content.

The diameter of composite yarns depends on the mass percentage of magnetic powder in the coating solution and is in the range of 427 μm to 465 μm for the coated yarns (see Table 3). Thus, the yarn diameter increases by 71 to 109 μm when compared to the 356 μm diameter of the reference (uncoated) yarn. The thickness of the magnetic layer and the density of the composite yarns are key parameters influencing the magnetic characteristics of the composite yarns. This in turn depends on the size of the magnetic particles, which in our case is in the range 0.54-1.64 μm (see Figure 8).

Since the range of magnetic particles diameter is large, it can have a noticeable influence on the tensile properties. Indeed, we observe that the increase in mass percentage of magnetic powder is initially leading to an increase in tensile properties up to a certain value. After this, we observe a decrease in tensile properties despite further increasing the mass percentage (Figures 12 and 13).

A statistical analysis has been employed in order to establish a relationship between the content of magnetic powder and tensile properties. As can be seen from Figures 12 and 13, a second-degree polynomial dependency exists between the barium hexaferrite mass percentage content and the tensile properties of the yarns. The value of the correlation coefficient illustrates a good and significant correlation (the value of R^2 is higher than 0.834.).

Figures 12 and 13 also reveal that the tensile strength of 6.25 N and the elongation at breaking of 10.07% of the support yarn increase for the composite yarn Y2 to 10.68 N and 15.54%, respectively. Starting with the

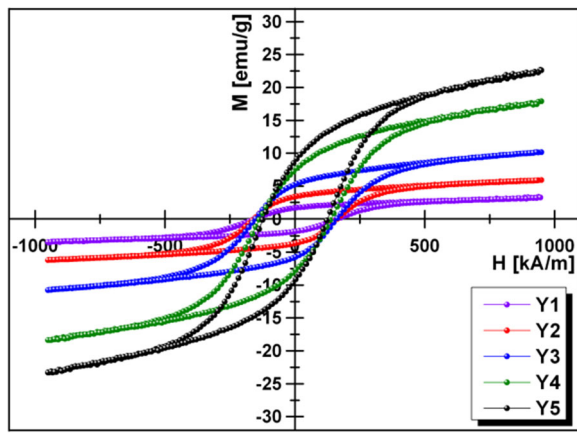


Figure 14. The hysteresis loops of magnetic samples magnetized by electromagnetic coil.

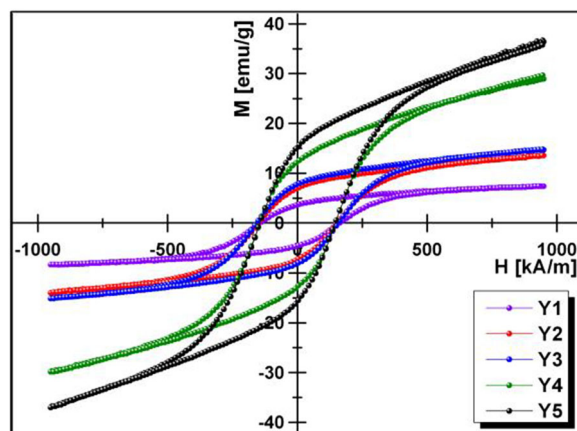


Figure 15. The hysteresis loops of magnetic samples magnetized by magnetic auger die.

Table 4. Experimental data of magnetic parameters depending on magnetic device.

Sample codes	Ferrite percentage content (%)	Toroidal coil		Magnetic auger die	
		Saturation induction (mT)	Residual induction (mT)	Saturation induction (mT)	Residual induction (mT)
Y1	10	6.53	3.25	13.04	6.47
Y2	20	11.43	6.59	26.32	13.59
Y3	30	19.67	10.23	28.49	15.18
Y4	40	34.68	14.53	56.11	23.96
Y5	50	48.51	22.26	78.47	32.90

composite yarn Y3, the tensile and elongation begin to decrease due to the increasing magnetic microparticle content. This can be attributed to two reasons: on one hand, the areas having higher powder concentrations break more easily; on the other hand, the expansion coefficients of the magnetic microparticles and the polymer materials in the coating solutions are different. Therefore, the lowest values of the tensile properties of the magnetic yarns were recorded at 50% barium hexaferrite mass percentage due to (i) the composite/magnetic yarn becomes too rigid and (ii) the magnetic particles penetrate in the structure of the support yarn, which can lead to structural discontinuities.

Another important parameter is the magnetization process used and the value of the magnetic field. Magnetic yarn samples of sufficient length were taken and placed perpendicular to the applied magnetic field lines on the magnetization devices depicted in Figure 3. The magnetic measurements performed on the samples are shown in Figures 14 and 15.

Our measurements in Figures 14 and 15 confirm that the magnetic yarns, i.e. cotton yarns covered with barium hexaferrite, are part of the hard magnetic materials because they present high values of the coercive field and low residual magnetization. Figures 14 and 15 also show that the residual magnetization and saturation are increasing with increasing amount of barium hexaferrite embedded in the textile yarns. The larger the ferrite percentage content the higher is the residual magnetization and saturation (see Table 4). For example, when comparing Y1 and Y5 samples, a five time increase in the ferrite content is resulting in an approximately seven times increase of the residual magnetization, i.e. from 3.25 mT to 22.26 mT for the electromagnetic coil. When comparing the Y1 and Y5 samples magnetized with permanent magnets, the residual magnetization is increasing about five times from 6.47 mT to 32.90 mT.

The values of the residual and saturation induction measured in the case of the 'auger' configuration are in most cases more than double as compared to those for the magnetic yarns magnetized with the electromagnetic coil. This aspect, which is also reflected in the hysteresis loops depicted in Figures 14 and 15 can be attributed to the fact, that hard magnetic ferrites have a history dependent non-linear response to external magnetic fields and the two magnetizing devices produce highly different fields (see Figure 3), both with respect to the maximum induction values and the spatial distribution.

Conclusions

In this study, we have produced and characterized magnetic single cotton yarns by employing two different indirect magnetization methods. The diameter of the coated yarns is directly dependent on the amount of magnetic powder in the coating solution. The magnetic yarn diameter increases with 30% when compared to the 356 μm diameter of the reference (uncoated) yarn for a barium hexaferrite mass percentage of 50%. SEM images of the coated yarns reveal a relatively uniform deposition of magnetic layer on the reference cotton yarn.

The tensile properties of composite yarns are increasing when compared to those of the reference yarn with the increase in barium hexaferrite mass percentage content

Two devices for the indirect magnetization of the coated yarns have been proposed. In both cases, the magnetic properties of the coated yarns (residual magnetism and coercive field intensity) are dependent on the amount of magnetic properties of the coated yarns is possible only by increasing the mass percentage of magnetic powder. However, we have observed differences in the magnetic properties of the yarns obtained using the two magnetization methods. Higher

values of residual field and saturation were measured after using the 'auger' magnetization device as compared to the electromagnetic coil.

Note

1. <https://greengraceusa.com/products/>

Disclosure statement

No potential conflict of interest was reported by the authors.

Funding

This work was supported by grant nr. 488PED/2020, TECHMAT, financed by Unitatea Executiva pentru Finantarea Invatamantului Superior, a Cercetarii, Dezvoltarii si Inovarii.

References

- Akman, O., Kavas, H., Baykal, A., Toprak, M. S., Çoruh, A., & Aktaş, B. (2013). Magnetic metal nanoparticles coated polyacrylonitrile textiles as microwave absorber. *Journal of Magnetism and Magnetic Materials*, 327, 151–158. <https://doi.org/10.1016/j.jmmm.2012.09.032>
- Akşit, A. C., Onar, N., Ebeoglugil, M. F., Birlik, I., Celik, E., & Ozdemir, I. (2009). Electromagnetic and electrical properties of coated cotton fabric with barium ferrite doped polyaniline film. *Journal of Applied Polymer Science*, 113(1), 358–366. <https://doi.org/10.1002/app.29856>
- Aldib, M. (2015). An investigation of an instrument-based method for assessing colour fastness to light of photochromic textiles. *Coloration Technology*, 131(4), 298–302. <https://doi.org/10.1111/cote.12156>
- Bartusch, M., Hetti, M., Pospiech, D., Riedel, M., Meyer, J., Toher, C., Neu, V., Gazuz, I., Shagolsem, L. S., Sommer, J.-U., Hund, R.-D., Cherif, C., Moresco, F., Cuniberti, G., Voit, B. (2014). Innovative molecular design for a volume oriented component diagnostic: Modified magnetic nanoparticles on high performance yarns for smart textiles. *Advanced Engineering Materials*, 16(10), 1276–1283. <https://doi.org/10.1002/adem.201400192>
- Bashir, T., Skrifvars, M., & Persson, N. K. (2011). Surface modification of conductive PEDOT coated textile yarns with silicone resin. *Materials Technology*, 26(3), 135–139. <https://doi.org/10.1179/175355511X13007211258926>
- Beica, T., Nistor, L. C., Morosanu, C., Frunza, L., Stan, G. E., Zgura, I., Marcov, D., Dorogan, A., Carpus, E. (2008). Studies on multifunctional textile materials. Plasma deposition onto textile materials and onto reference plates. *Journal of Optoelectronics Advanced Materials*, 10, 2811–2817.
- Campos, I., Lucas, J., Gil, H., Miguel, R. A. L., Trindade, I., & Santos, S. M. (2011). Development of textile substrates with magnetic properties. In Autex Conference, Mulhouse, France (pp. 773–777).
- Chowdhury, B., M.A., Butola, B. S., & Joshi, M. (2013). Application of thermochromic colorants on textiles: Temperature dependence of colorimetric properties. *Coloration Technology*, 129(3), 232–237. <https://doi.org/10.1111/cote.12015>
- Ghosh, S., Remanan, S., Mondal, S., Ganguly, S., Das, P., Singha, N., & Das, N. C. (2018). An approach to prepare mechanically robust full IPN strengthened conductive cotton fabric for high strain tolerant electromagnetic interference shielding. *Chemical Engineering Journal and the Biochemical Engineering Journal*, 344, 138–154. <https://doi.org/10.1016/j.cej.2018.03.039>
- Grosu, M. C., Lupu, I. G., Cramariuc, O., & Hogas, H. (2018). Fabrication and characterization of magnetic cotton yarns for textile applications. *The Journal of the Textile Institute*, 109(10), 1348–1359. <https://doi.org/10.1080/00405000.2018.1423935>
- Grosu, M. C., Lupu, I. G., Cramariuc, O., & Hristian, L. (2016). Magnetic cotton yarns – optimization of magnetic properties. *The Journal of the Textile Institute*, 107(6), 757–765. <https://doi.org/10.1080/00405000.2015.1061761>
- Hemapriyamvadhya, R., & Sivasankar, T. (2015). Sonophotocatalytic treatment of methyl orange dye and real textile effluent using synthesised nano-zinc oxide. *Coloration Technology*, 131(2), 110–119. <https://doi.org/10.1111/cote.12139>
- Jia, L.-C., Xu, L., Ren, F., Ren, P.-G., Yan, D.-X., & Li, Z.-M. (2019). Stretchable and durable conductive fabric for ultrahigh performance electromagnetic interference shielding. *Carbon*, 144, 101–108. <https://doi.org/10.1016/j.carbon.2018.12.034>
- Joseph, J., & Stupak, J. (2000). Methods of Magnetizing Permanent Magnets, EMCW Coil Winding Show 1 October-2 November 2000, Cincinnati, Ohio.
- Kang, T. J., Choi, A., Kim, D. H., Jin, K., Seo, D. K., Jeong, D. H., Hong, S., Park, Y. W., & Kim, Y. H. (2011). Electromechanical properties of CNT-coated cotton yarn for electronic textile applications. *Smart Materials Structure*, 20(1).
- Koby, M., Gengec, E., Sensoy, M. T., & Demirbas, E. (2014). Treatment of textile dyeing wastewater by electrocoagulation using Fe and Al electrodes: Optimisation of operating parameters using central composite design. *Coloration Technology*, 130(3), 226–235. <https://doi.org/10.1111/cote.12090>
- Loss, C., Gonçalves, R., Pinho, P., & Salvado, R. (2019). Influence of some structural parameters on the dielectric behavior of materials for textile antennas. *Textile Research Journal*, 89(7), 1131–1143. <https://doi.org/10.1177/0040517518764000>
- Petrla, I., & Tudorache, F. (2014). Influence of partial substitution of Fe³⁺ with W³⁺ on the microstructure, humidity sensitivity, magnetic and electrical properties of barium hexaferrite. *Superlattices and Microstructures*, 70, 46–53. <https://doi.org/10.1016/j.spmi.2014.02.014>
- Rubacha, M., & Zięba, J. (2006). Magnetic textile elements. *Fibres Text East Europe*, 14, 48–52.
- Sözeri, H., Durmuş, Z., Baykal, A., & Uysal, E. (2012). Preparation of high quality, single domain BaFe₁₂O₁₉ particles by the citrate sol-gel combustion route with an initial Fe/Ba molar ratio of 4. *Materials Science and Engineering: B*, 177(12), 949–955. <https://doi.org/10.1016/j.mseb.2012.04.023>
- Vinnik, D. A., Zhrebtsov, D. A., Mashkovtseva, L. S., Nemrava, S., Yakushechkina, A. K., Semisalova, A. S., Gudkova, S. A., Anikeev, A. N., Perov, N. S., Isaenko, L. I., Niewa, R. (2015). Tungsten substituted BaFe₁₂O₁₉ single crystal growth and characterization. *Materials Chemistry and Physics*, 155, 99–103. <https://doi.org/10.1016/j.matchemphys.2015.02.005>
- Wiak, S., Firyach-Nowacka, A., & Di Barba, P. (2012). Computer homogeneous models and magnetization curve of magnetic micro-fibers. *COMPEL - The International Journal for Computation and Mathematics in Electrical and Electronic Engineering*, 31(5), 1521–1527. <https://doi.org/10.1108/03321641211248273>
- Wiak, S., Firyach-Nowacka, A., & Smolka, K. (2010). Computer models of 3D magnetic microfibres used in textile actuators. *COMPEL - The International Journal for Computation and Mathematics in Electrical and Electronic Engineering*, 29(5), 1159–1171. <https://doi.org/10.1108/03321641011061380>
- Xu, B., Eike, R. J., Cliett, A., Ni, L., Cloud, R., & Li, Y. (2018, December). Durability testing of electronic textile surface resistivity and textile antenna performance. *Textile Research Journal*, 89(18). <https://doi.org/10.1177/0040517518819848>
- Zieba, J. (2007). Models of textile magnetic core. *RJTA*, 11(4), 87–92.
- Zieba, J., Grosu, M. C., & Frydrysiak, M. (2011). Simulation of yarns textile magnetic core; STRUTEX, TU Liberec. Paper Conference, The 18-th International Conference, Czech Republic, 375–378.